

EMI prediction method for SiC inverter by the modeling of structure and the accurate model of power device

Sari Maekawa, Junichi Tsuda, Atsuhiko Kuzumaki,
 Shuhei Matsumoto, Hiroshi Mochikawa
 TOSHIBA CORPORATION FUCHU OPERATIONS
 1, Toshiba-Cho, Fuchu-Shi, Tokyo, Japan 183-8511
 sari1.maekawa@toshiba.co.jp

Hisao Kubota
 Graduate School of Science and Technology,
 Meiji University
 1-1-1 Higashimita, Tamaku, Kawasaki, 214-8571, JAPAN
 kubota@isc.meiji.ac.jp

Abstract— In recent years, the switching speed is increased acceleratedly. And, the increase of EMI by high dv/dt is a problem. In this paper, the Tri-phase 400 V_{rms} inverter for system interconnections which used SiC-JFET is analyzed. And, it is shown that noise terminal voltage is analyzable with an error of ± 15 dB by highly precise modeling.

Keywords— EMI, analysis, power electronics, SiC.

I. INTRODUCTION

In recent years, to reduce a switching loss, a switching speed is dramatically increased. The increase of Electro Magnetic Interference (EMI) by high gradient of time may causes improper operation of neighbor devices.

For the above reason, it is necessary to reduce EMI by a noise filter. In order to estimate EMI in a design phase before a trial production, highly precise EMI analysis technology is required. Estimating EMI for power electronics are studied by high precise analytical modeling [1-6], and the modeling including parasitic components with electromagnetic-field analysis in recent years [1-18].

In this paper, Tri-phase 400 V_{rms} inverter for system interconnections with SiC-JFET is analyzed. The frequency range is from 150 kHz to 30 MHz specified by CISPR11 Class A [19]. The study achieved that the noise terminal voltage is analyzable with an error of ± 15 dB by high precise modeling.

II. COMPOSITION OF THE INVERTER OF ANALYSIS OBJECT

A. Composition of an EMI evaluation system

Fig.1 is the evaluation system of noise terminal voltage, and Fig.2 is experimental setup for measuring conducted EMI. The evaluation system consists of a DC power supply, an inverter, a normal mode filter, and load resistance. And, in order to measure noise terminal voltage, LISN is added between an inverter and load resistance. The inverter of this paper is targeting system interconnections, such as photovoltaic generation. Output

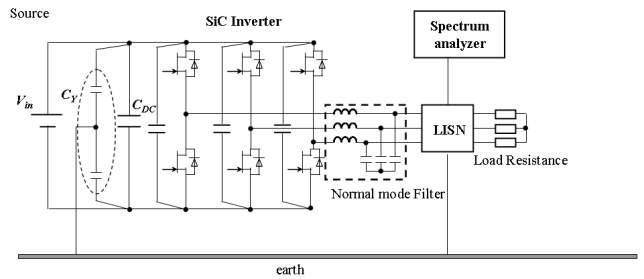


Fig. 1. Evaluation system configuration of conducted.

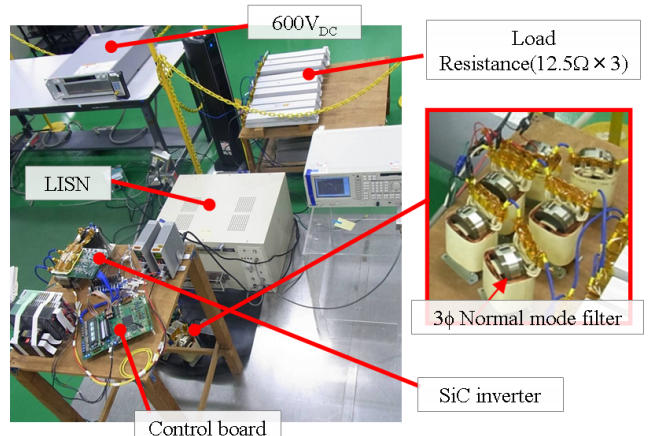


Fig. 2. Experimental setup for measuring conducted EMI.

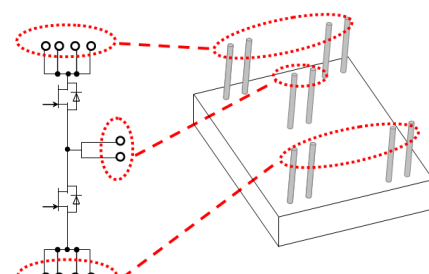


Fig. 3. Illustration of a half-bridge module.

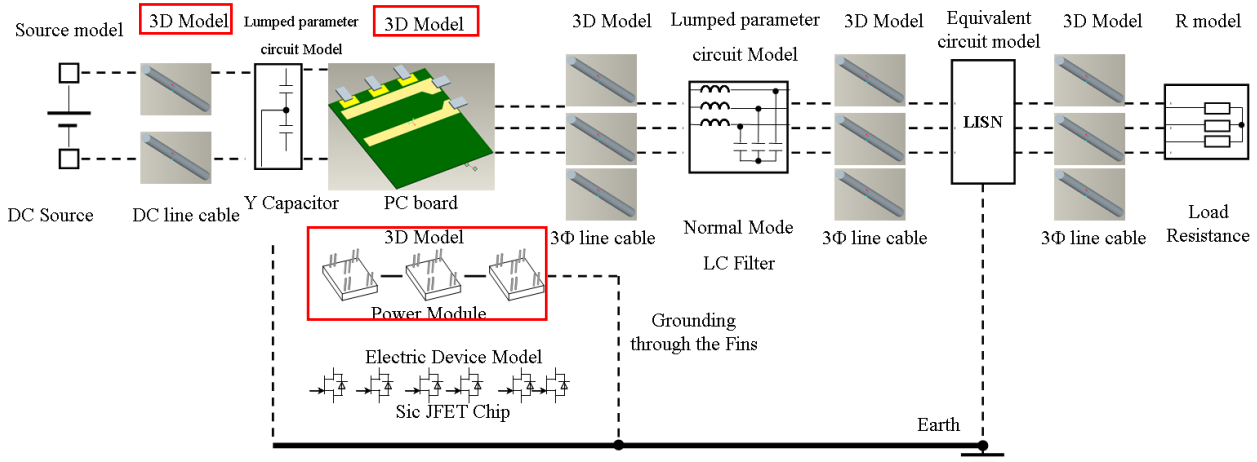


Fig. 4. Modeling structure of the evaluation system.

rating is tri-phase 400V_{rms} and 10 kW.

B. Composition of a main circuit

Main circuit composition is 3-phase inverter of two levels. The inverter uses three half bridge modules shown by Fig.3.

III. MODELING OF THE INVERTER IN EMI ANALYSIS

A. The outline of modeling

Fig.4 shows the modeling composition of the evaluation system.

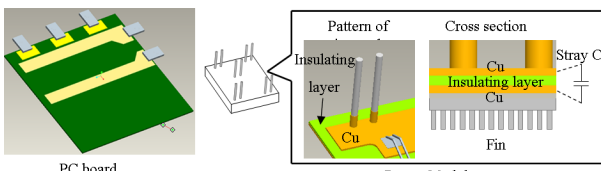
The parasitic components generated according to the structure of the circuit (ex. printed circuit board, power module). For this reason, a parasitism components is extracted from these by conducting electromagnetic-field analysis of the 3-D model.

The device model which reproduced the switching characteristic is used for the SiC chip mounted in a power module.

The frequency characteristic of the impedance of a reactor and a capacitor is reproduced in the equivalent circuit by a lumped constant.

B. Modeling of a printed circuit board, a power module, and a cable

The pattern of the DC section and the UVW section is modeled in the printed circuit board. Furthermore, the composition between the layers of a pattern is also modeled. As for a power module, an internal circuit pattern is modeled. And, the layer composition to the



(a) Model of the circuit board (b) Model of the power module
Fig. 5. Illustration of the (a) PC board and (b) power module of the inverter.

radiating fin is modeled. Since a radiating fin is grounded to Earth in Fig.4, the modeling of the stray capacitance between a SiC device and a fin is important. The 3-D model of a printed circuit board is shown in Fig.5 (a), and the 3-D model of a power module is shown in (b). The parasitic components are extracted from each model and it outputs as an equivalent circuit of LCR as shown in Fig.7. Furthermore, they are combined on a circuit simulator (Fig.6). In the equivalent circuit, the resistance R , stray capacitance C , and inductance L,M between each node of a model are taken into consideration.

In addition, the parasitic components is extracted with BEM(Boundary Element Method) by Q3DExtractor of ANSYS. Circuit analysis is using Simplorer of ANSYS.

TABLE.I shows the parasitism components of Sic module. The parasitism components shown in TABLE.I is the stray capacitance between a installation part of a fin

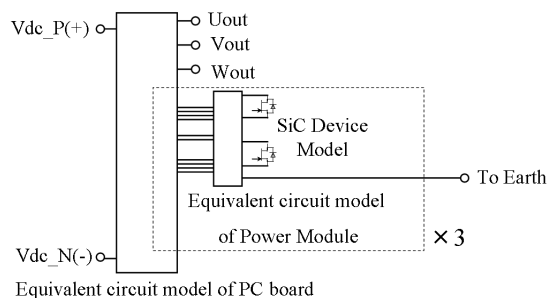


Fig. 6. Reflect on the circuit simulator.

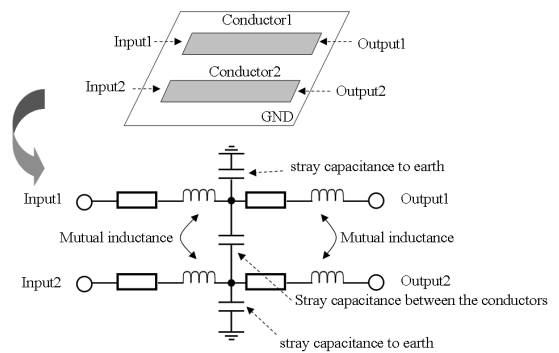


Fig. 7. Equivalent circuit of the parasitic components.

TABLE I. Comparison of the stray capacitances of analysis and measurement

Part	Analysis Capacitance [pF]	Measurement Capacitance [pF]
V_{DCP} to Fin	79	-
V_{DCN} to Fin	66	-
Output to Fin	74	-
Sum	219	202

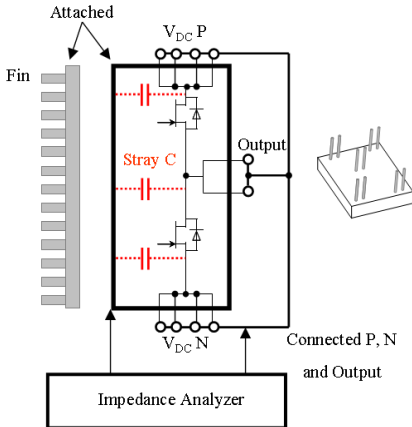


Fig. 8, Experimental setup for measurement stray capacitances of SiC module

and each part. The measuring method of stray capacitance is shown in Fig. 8. The terminal of V_{DCP} , V_{DCN} and Output are connected, and the stray capacitance is measured with the impedance analyzer. The output capacitance C_{ds} of SiC JFET is very large compared with stray capacitances, when V_{ds} is small. Therefore, it is difficult to measure the stray capacitances of each part correctly.

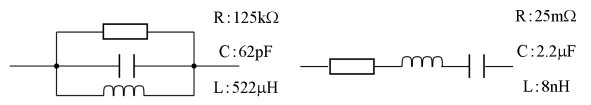
C. Modeling of a capacitor and reactor

The normal mode filter which consists of a reactor and a capacitor is connected to the output of an inverter. The frequency characteristic of L , C , and R which constitute a filter is important in the frequency range (150kHz-30MHz) of the CISPR11 class A. For this reason, the model is using the lumped constant circuit.

Fig.9 shows the lumped constant circuit and value of the normal mode filter (reactor, capacitor). Fig.10 (a) shows the frequency characteristic of the reactor. In contrast, Fig.10 (b) shows that for capacitor. The frequency characteristic is reproducible. Other capacitors are modeled similarly. The resistor for loads shown by Fig.1 is expressed only by R .

D. Modeling of LISN

LISN is a circuit which measures noise terminal voltage. The equivalent circuit shown by the maker is used. Fig.11 shows the equivalent circuit of LISN in an evaluation system. The terminal point to Earth are LISN, Y capacitor of DC part, and the radiating fin of a power module, as shown in Fig.4.



(a) Reactor (b) Capacitor
Fig. 9. Equivalent circuit of the (a) reactor and (b) capacitor.

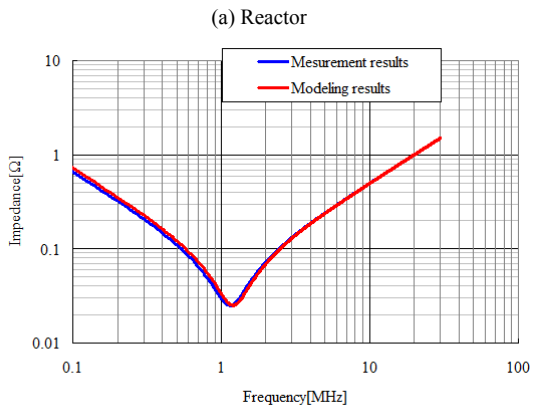
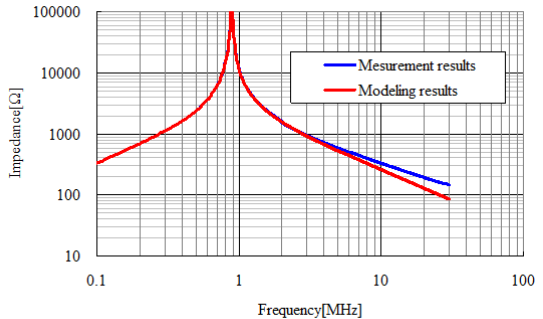


Fig.10. Impedance vs frequency plot for the (a) reactor and (b) capacitor.

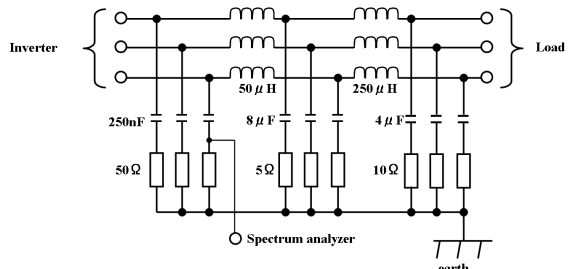


Fig. 11. Equivalent circuit of the LISN.

E. Modeling of SiC power device

In this paper, a SiC power device is switched on condition of high dv/dt . For this reason, the switching characteristic of a SiC is important, and the characteristic is expressed by the equivalent circuit model shown in Fig.12. Although a power device is JFET, the characteristic of normally on of JFET is expressed in the MOSFET model with negative gate threshold voltage. The resistance and inductance which are connected to gate, drain, and source are parasitic components in a chip. The parasitic components in a power module are

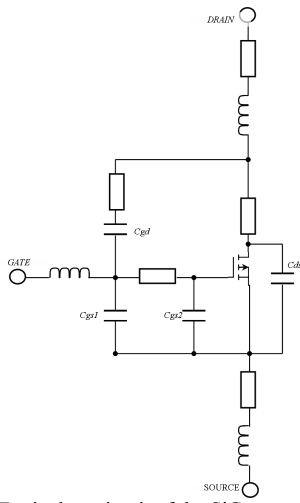


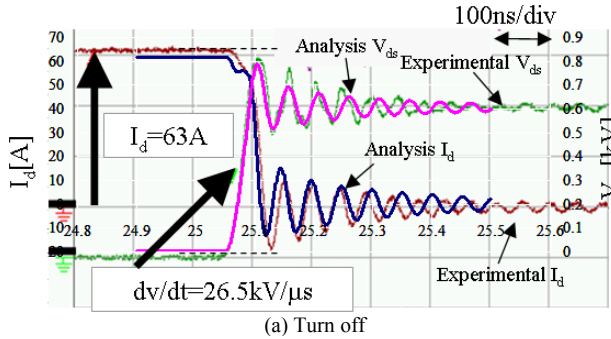
Fig. 12. Equivalent circuit of the SiC power devices.

expressed by (II. B).

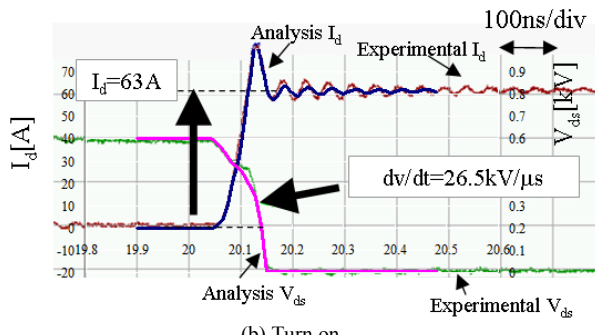
The switching characteristic is expressed by modeling V_{gs} - I_d and V_{ds} - I_d as a static characteristic, and modeling the characteristic of C_{gs} , C_{gd} , and C_{ds} as dynamic characteristics. The accuracy of the waveform of V_{ds} is improved by changing each capacitance by ON/OFF of SiCJFET [20,21]. Each capacitance has determined from the experimental result of the switching waveform.

The reverse-recovery characteristics of a diode are as important as the switching characteristic, and it is expressing them using the device level diode dynamic-characteristics model of ANSYS Simplorer [22]. As a result, the characteristic of recovery-current is reproducible.

Fig.13 shows the switching waveform of SiCJFET which modeled the switching characteristic (static and



(a) Turn off



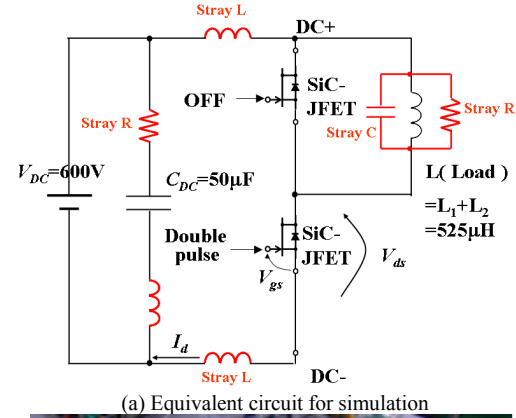
(b) Turn on

Fig. 13. Reproducibility of switching characteristics at (a) turn off and (b) turn on.

dynamic) and reverse-recovery characteristics.

The experiment uses the double pulse circuit shown by Fig.14(a)(b). Parasitism components, such as stray inductance and stray capacitance are added to the simulation circuit to compare in Fig.14(a). SiCJFET uses the module shown by Fig.3.

In Fig.13, the dv/dt of V_{ds} is reproduced by modeling of a static characteristic and dynamic characteristics.



(a) Equivalent circuit for simulation

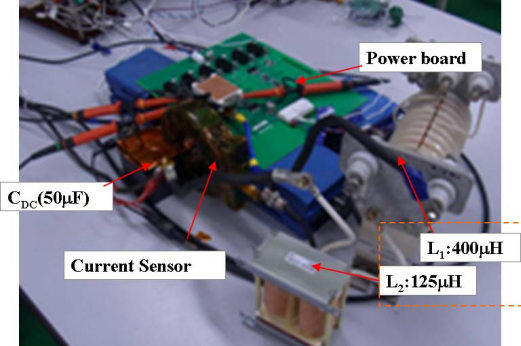
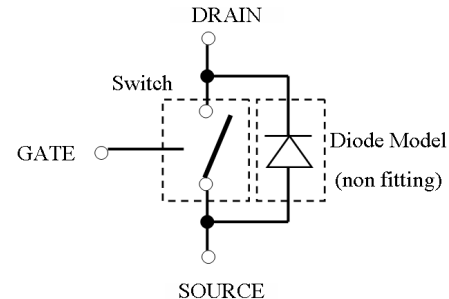

 (b) Experimental setup
Fig. 14. Configuration of the double-pulse test circuit.


Fig. 15. Simulation and experimental results of the noise voltage in frequency

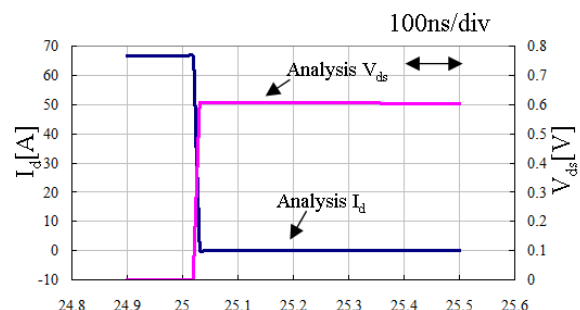


Fig. 16. Characteristics of the ideal switch model (OFF).

Although I_d and V_{ds} waveform at the time of turn-on are greatly influenced by the recovery characteristic in a double pulse examination, the accuracy of estimation by a simulation is good.

In contrast, when it does not model the switching characteristic and reverse recovery characteristics shown in Fig.15, a turn-off becomes a waveform as shown in Fig. 16. This uses the simple switch model. In a simple switch model, since the characteristics of capacitance differ, dv/dt of V_{ds} is higher than the experimental result.

IV. SIMULATION RESULTS

A. Estimation of noise terminal voltage

As a result of our analysis, noise terminal voltage is obtained by a model with following items. The model consists of equivalent circuits of parasitism components in each part of our test inverter, reactors and capacitors modeled as lumped constant circuit, and characteristics of SiC power devices.

Fig.17 shows Fast Fourier Transform (FFT) of simulation and experimental results of noise terminal voltage in the case of modeling above all components. Compared to an experimental result, our proposed method achieves to estimate EMI with an error of ± 15 dB in frequency range from 150 kHz to 30 MHz specified in the CISPR11 class A.

B. The influence of accurate model of power device

The power device of an inverter is SiC and its dv/dt is high. Fig.18 shows the difference arising from a power device model. The simply power device model is a model shown in Fig. 15 and Fig.16. The accurate model is reproducing static characteristics, dynamic characteristics and reverse recovery characteristics. The difference has appeared from the frequency of over 5 MHz. Since dynamic characteristics is not reproduced enough, the simply power device model has quick switching.

As a result, the frequency of dv/dt became high and the difference appeared in EMI.

V. CONCLUSION

(1)This paper investigates EMI analysis for SiC inverter.
(2)This paper modeled following items: parasitism

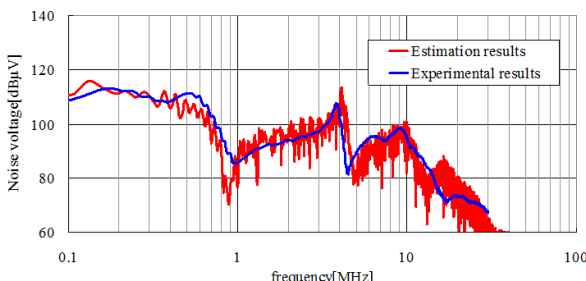


Fig. 17. Simulation and experimental results of the noise voltage in frequency

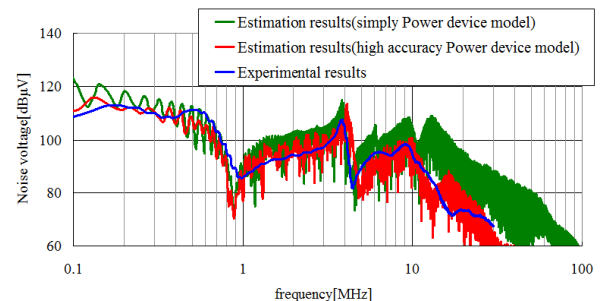


Fig. 18. Simulation and experimental results of the noise voltage in frequency

components of our test inverter circuit, frequency characteristics of passive components, and switching characteristics of SiC power device.

- (3)As a result, our proposed method achieves to estimate EMI with an error of ± 15 dB in frequency range from 150 kHz to 30MHz specified in CISPR11 class A.
- (4)This paper considers a modeling method for three circuit components in EMI analysis for SiC inverter. The study verifies an accuracy of our model by experiments of switching test, EMI measurement, and impedance measurement.

REFERENCES

- [1] R. Kraus, P. Türkcs, J. Sigg : "Physics-based models of power semiconductor devices for the circuit simulator SPICE", *Power Electronics Specialists Conference*, 1998. PESC 98 Record. 29th Annual IEEE, Vol. 2, pp. 1726-1731(1998)
- [2] Allen R. Hefner, Daniel M. Diebolt : "An experimentally verified IGBT model implemented in the Saber circuit simulator", *IEEE Transactions on Power Electronics*, Vol. 9, No. 5, pp. 532-542 (1994)
- [3] N. Okada, T. Kikuma, M. Takasaki, K. Kodani, A. Kuzumaki : "Development of Device Model for Inverter Simulation Program" , *Industrial Application Conference of IEEJ*, No.1-131, pp. 515-520 (2008) (in Japanese)
- [4] A. Hatanaka, T. Kawashima, A. Mishima : "Analysis technique of EMC for on-board power supply with recovery diode model" , *Industrial Application Conference of IEEJ*, No. 1-132, pp. 525-528 (2008) (in Japanese)
- [5] Y. Iwata, S. Tominaga, H. Fujita, F. Akagi, T. Horiguchi, S. Kinouchi, T. Oi, H. Urushibata : "Investigation of noise and switching-energy loss by using a precise MOSFET model" , *Industrial Application Conference of IEEJ*, No. 1-135, pp. 615-618 (2011) (in Japanese)
- [6] A. Mishima, T. Kawashima : "Switching analysis methods using Power Device Model and Magnetic Field Coupling System", *Industrial Application Conference of IEEJ*, No. 1-S7-5, pp. 95-100 (2003) (in Japanese)
- [7] Y. Koyama, M. Tanaka, H. Akagi : "Modeling and Analysis for Simulation of Common-Mode Noises Produced by an Inverter-Driven Air Conditioner", *Industrial Application Conference of IEEJ*, No.1-O2-5, pp.175-180 (2009) (in Japanese)
- [8] T. Shimizu, G. Kimura, J. Hirose : "High Frequency Leakage Current Caused by the Transistor Module and Its Suppression Technique", *T. IEE Japan*, Vol. 116-D, No. 7, pp. 758-766 (1966) (in Japanese)
- [9] J.-S.Lai, X. Huang, E. Pepa, S.Chen, and T.W.Nehl : "Inverter EMI Modeling and Simulation Methodologies", *Proceedings of 29th Annual Conference of the IEEE Industrial Electronics Society*, Vol. 2, pp. 1 533-1539 (2003)
- [10] B. Revol, J. Roudet, J.L. Schanen, and P. Loizelet : "Fast EMI Prediction method for three phase inverter based on Laplace

- Transforms”, *Proceedings of 34th IEEE Annual Power Specialists Conference*, Vol. 3, pp. 1133-1138 (2003)
- [11] M. Tamate, T. Sasaki, A. Toba : “Quantitative Estimation of Conducted Emission from an Inverter System”, *T. IEE Japan*, Vol. 128-D, No. 3, pp. 193-200 (2008) (in Japanese)
- [12] S. Ogasawara : “Modeling and Simulation of EMI in Power Electronics systems”, *Industrial Application Conference of IEEJ*, 1-S11-2, pp.69-74 (2004) (in Japanese)
- [13] A. Okuno, S. Ogasawara : “Simulation in Power Electronic Systems-Characteristics of General-Purpose Simulators and System Modeling Methods”, *T. IEE Japan*, Vol.122-D, No. 9, pp. 893-898 (2002) (in Japanese)
- [14] Y. Kondo, M. Izumichi : “VHF conducted emission simulation of power electronic devices”, *Industrial Application Conference of IEEJ*, No. 1-40, pp. 205-208 (2012) (in Japanese)
- [15] [15] T. Koga, K. Shigematsu, S. Hasumura: “A Study of common mode current reduction in PWM inverter with core modeling and circuit simulation”, Annual Conference of IEEJ, No. 4-019, p. 33 (2009) (in Japanese)
- [16] T. Chida, A. Mishima, T. Kamezawa, K. Mou, S. Ibori : “Analysis of conducted emission in general purpose inverter”, Industrial Application Conference of IEEJ, No. 1-38, pp. 299-300 (2007) (in Japanese)
- [17] G. Xun, J. A. Ferreira : “Investigation of Conducted EMI in SiC JFET Inverters Using Separated Heat Sinks”, *IEEE Transactions on Industrial Electronics*, Vol. 61, No. 1, pp. 115-125 (2014)
- [18] W. Junsheng, D. Gerling, S. P. Schmid : “Prediction of conducted EMI in power converters using numerical methods”, Proceedings of Power Electronics and Motion Control Conference (EPE/PEMC) 2012 , DS1a.3-1 - DS1a.3-6 (2012)
- [19] IEC CISPR 11 Edition.5.0: Industrial, scientific and medical equipment – Radio-frequency disturbance characteristics – Limits and methods of measurement, IEC Standard, May, 2009.
- [20] T. Sekisue(ANSYS JAPAN): “Parameter for SIMPLORER’s IGBT device model”, ANSYS JAPAN user support documents.(2010) (in Japanese)
- [21] J. Aurich, T. Barucki, : “Fast dynamic model family of semiconductor switches”, Power Electronics Specialists Conference, 2001. PESC 2001 Record. 32th Annual IEEE, Vol. 1, pp. 67-74 (2001)
- [22] T. Sekisue(ANSYS JAPAN): “Parameter fitting for SIMPLORER’s device model starting with diode characteristics”, ANSYS JAPAN user support documents. (2009)(in Japanese)